

THE IMPORTANCE OF SEASONAL SEA-LEVEL VARIATIONS FROM GEOPHYSICAL MODELS AND SATELLITE GRAVIMETRY FOR EXCITATION OF LENGTH-OF-DAY

R. DILL, H. DOBSLAW

GFZ, Sec. 1.3 Earth System Modelling, Dep. 1 - Germany
dill@gfz-potsdam.de, dobslaw@gfz-potsdam.de

ABSTRACT. In addition to atmospheric, oceanic, and hydrological contributions, the seasonal length-of-day variation is significantly affected by global mass redistribution between the Earth subsystems. This study uses the new ESMGFZ barystatic sea-level product SLAM as well as estimates of the barystatic ocean bottom pressure anomalies from the GRACE Level 3 GravIS products to quantify the global mass balance. For the annual cycle the global mass balance effect overcompensates the contributions from terrestrial hydrology. Considering the global mass balance, model based mass induced excitation on seasonal length-of-day variations coincide well with estimates from satellite gravimetry. Moreover, the mass terms can be determined accurate enough to attribute the remaining gap in the length-of-day excitation budget between models and observation clearly to an underestimation of atmospheric wind speeds in the global European weather forecast model by -7%.

1. INTRODUCTION

On seasonal time-scales changes in length-of-day (ΔLOD) are mainly caused by external gravitational forces, the redistribution of water masses within Earth's fluid layers atmosphere, ocean, and terrestrial hydrosphere, and the exchange of water masses between these components. Models of the hydrosphere dynamics, i.e., numerical weather prediction models, ocean general circulation models, and terrestrial water storage models can be used to calculate effective angular momentum functions (EAM) describing the excitation of Earth rotation. Atmospheric angular momentum (AAM) consisting of wind and surface pressure changes account for almost 90 % of observed ΔLOD . To a smaller extent ΔLOD is excited by terrestrial hydrology (HAM) and the exchange of water masses between the continents and the ocean responsible for the seasonal sea-level changes (SLAM). The global mass balance, expressed as sea-level variation including effects of loading and self-attraction is generally not included in the available EAM data sets.

2. BARYSTATIC SEA-LEVEL CHANGES

Barystatic sea-level changes are induced by the net-inflow of water from the continents or the atmosphere into the oceans and by a spatially variable deformation of an equipotential surface of the Earth's gravity field that coincides with the sea-surface on a global average. Ocean mass variations can be directly extracted from gravity variations from the Gravity Recovery and Climate Experiment GRACE (2002 - 2017) and GRACE-FO (launched on May 22nd, 2018), e.g. latest GRACE reprocessing release 06 performed at GFZ (Dahle et al., 2018), publicly available from the GravIS portal (gravis.gfz-potsdam.de).

Alternatively, barystatic sea-level changes can be calculated from global water balance assuming that the total mass of water on the globe is constant in time. Gravitationally consistent spatially heterogeneous sea-level variations can be deduced by solving the so-called sea-level equation. Based on daily estimates of the ESMGFZ models of the atmosphere (i.e., global ECMWF analysis and re-analysis data) and the continental hydrosphere (i.e., Land Surface Discharge Model LSDM),

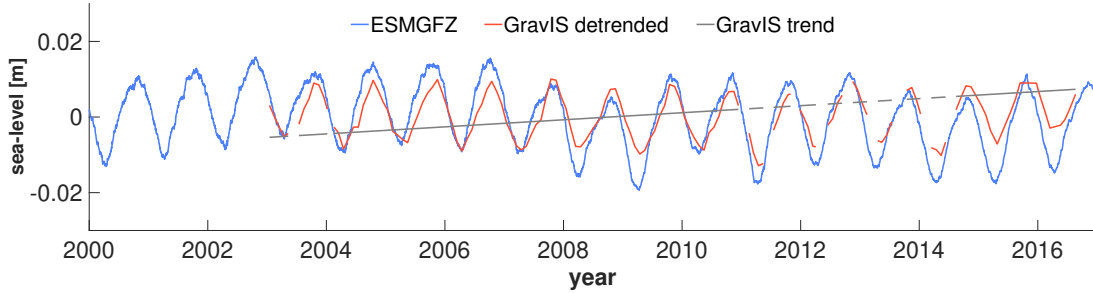


Figure 1: Barystatic sea-level variations for the years 2000 - 2016 in [m]. Blue: 24-hourly sea-level calculated from atmospheric and hydrological mass changes in the ESGFZ models ECMWF and LSDM by solving the sea-level equation. Red: Monthly GRACE based sea-level variation from GravIS Barystatic Pressure Anomalies, detrended. Gray: Removed trend of GravIS Barystatic Pressure Anomalies.

we note that, apart from the trend, both signals agree very well even on interannual time-scales (Figure 1). The annual amplitude of the barystatic sea-level changes inferred from the ESGFZ models is about 5% higher than the most recent GRACE estimate from GFZ, and the phase difference is about 7 days. ESGFZ does not account for post-glacial rebound.

3. EFFECTIVE ANGULAR MOMENTUM FUNCTIONS

Effective Angular Momentum (EAM) functions (χ_1, χ_2, χ_3) summarize the geophysical excitation of Earth rotation. Each EAM function consists of so-called mass terms induced by mass redistributions, and motion terms caused by mass transports associated with atmospheric winds and ocean currents. The axial component χ_3 quantifies ΔLOD . Global numerical models allow for the separate quantification of atmospheric angular momentum changes AAM, oceanic angular momentum OAM, and hydrological angular momentum HAM. Alternatively, satellite geodesy allows for the quantification of the total excitation from the inversion of the Earth Orientation Parameters as available from in particular geometric techniques, and additionally also for the estimation of the total mass term from the analysis of gravimetric observations.

3.1 Model-based AAM, OAM, HAM, and SLAM

Since more than 10 years, the Earth System Modelling group at GFZ Potsdam (ESMGFZ) provides daily updated EAM functions as calculated from numerical model data. Since the beginning of 2017 ESGFZ provides in addition so-called barystatic Sea-Level Angular Momentum functions (SLAM) that account for the GMB consistent to their models used for the calculation of AAM, OAM, and HAM. SLAM is calculated from the global distributions of modeled atmospheric and terrestrial water storage masses by means of the sea-level equation (Tamisiea et al., 2010). SLAM thus balances the global mass in the model system in a way that the sum of the total mass in all four different EAM components is constant at any time. SLAM represents mainly the hydrological and atmospheric excess mass distributed globally into the ocean but includes also the gravimetric effect of loading and self-attraction acting on the ocean sea-level.

Alternative model-based EAM time-series for this study were taken from the Global Geophysical Fluids Center (GGFC) of the International Earth Rotation and Reference Systems Service (IERS). AAM from Atmospheric and Environmental Research (AER) based on the Reanalysis-2 of the National Center for Environmental Prediction and OAM from the Jet Propulsion Laboratory (JPL) using the ocean model ECCO version kf080h.

3.2 Mass Terms from SLR and GRACE

Mass terms of the total excitation χ_3 are directly related to time-variations of the second degree zonal coefficient ΔC_{20} of the Earth's gravity field via the MacCullag's formula. We utilize ΔC_{20} from a multi-satellite Satellite Laser Ranging (SLR) solution (SLR_Multi) as provided by the Center for Space Research (Cheng et al., 2011). We further consider the annual amplitudes and phases obtained from a comparable SLR analysis setting reported by Zhang (2017) noted as SLR_Zhang. Thirdly, we use a SLR series that has been specifically calculated to replace ΔC_{20} in the GRACE RL06 series as published in the GRACE TN11 (SLR_TN11; Cheng et al., 2013). Fourthly, we test an SLR-series processed at GFZ that considers in total six different satellites (SLR_GFZ; Koenig et al., 2018).

In addition, the Gravity Information Service website <http://gravis.gfz-potsdam.de/> (GravIS) provides a preliminary separation of the ocean gravity signal observed by GRACE into the part induced by general circulation pressure anomalies and the GMB part induced by barostatic pressure anomalies. From the latter mass distribution we can derive a SLAM products that relies almost purely on observations from GRACE.

3.3 GAM from IERS C04

The geodetic angular momentum function (GAM) is inverted from the geodetically observed Earth's rotation time series IERS EOP 14 C04 by means of the Liouville equation. Effects of long-period tides were removed from the GAM ΔLOD component.

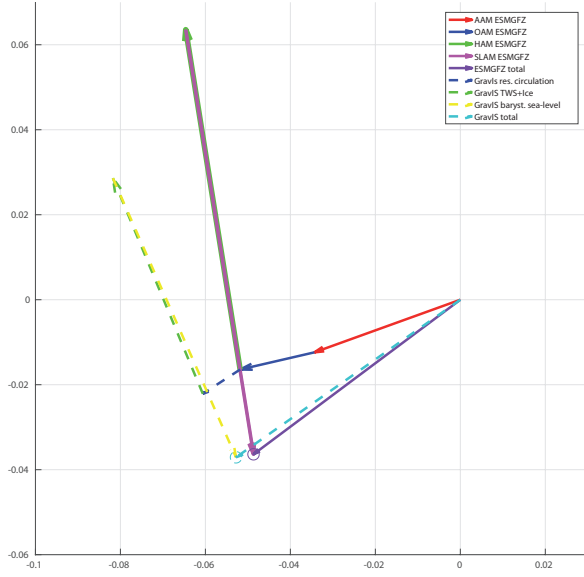
4. ANNUAL MASS TERM VARIABILITY

We initially focus on the effects of the quasi-static mass distribution on the annual and semi-annual harmonic in ΔLOD excitation. We estimated a least squares harmonic fit to the angular momentum time series with bias, trend, annual, semi-annual, and ter-annual harmonics.

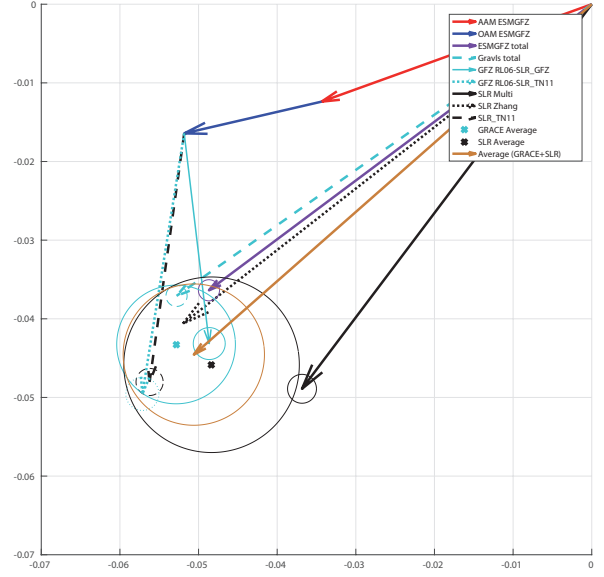
The sum of all model-based ESMGFZ EAM coincides quite well with the total GRACE-based contribution as given by GravIS (Figs. 2a). Annual OAM mass term contributions are well in phase with the atmospheric mass excitations. Residual ocean bottom pressure variability observed by GRACE indicates that MPIOM is still missing a considerable fraction (35%) of the excitation.

For both, ESMGFZ and GravIS, HAM is overcompensated by SLAM with a 24% larger magnitude. SLAM arises by 82% from the hydrological balance, 16% from the atmospheric balance, and 2% from the gravitational effects of atmospheric and continental water masses on the sea-level topography.

The comparison of SLR_TN11 with the GRACE solution GFZ RL06-SLR_TN11 including a replaced C_{20} estimate from SLR_TN11 confirms that numerical integration of EAM from global mass grids obtained with GRACE is sufficiently accurate and do not affect the results (Figs. 2b). In contrast, the choice of an particular SLR solution for the C_{20} replacement in the GRACE level 2 processing significantly impacts the results, see differences between GFZ RL06-SLR_TN11 and GFZ RL06-SLR_GFZ. Considering all three GRACE based solutions, the annual mass term is determined with an accuracy of $\pm 0.9 \cdot 10^{-10}$ in amplitude and $\pm 3.7^\circ$ in phase. The SLR solutions reveal a somewhat larger deviation from each other, $\pm 1.3 \cdot 10^{-10}$ in amplitude and $\pm 8.1^\circ$ in phase. The unweighted mean of the three SLR solutions leads to almost the same annual mass term signal as the GRACE average estimate. Moreover, the result from the ESMGFZ model fit also quite well within the distribution of all considered geodetic estimates. We thus conclude that the mass terms of annual ΔLOD excitations is fairly well understood from a combination of satellite gravimetry and numerical models.



(a) Phasor plot of annual mass term contribution χ_3 mass, part 1. Individual contributions from atmosphere (red), ocean (blue), terrestrial hydrology (green), and barystatic sea-level (pink ESMGFZ, yellow GravIS) as well as the sums (purple ESMGFZ, turquoise GravIS) are given for the model ESMGFZ (solid lines) and GRACE L3 product GravIS (dashed lines). Circles represent the uncertainties in estimating the annual harmonic signal. Amplitudes are in milliseconds, phases are defined as φ in $\sin(\omega(t - t_0) + \varphi)$, where t_0 refers to 0 UTC on January 1 and $\omega = 1/365.25d$.



(b) Phasor plot of annual mass term contribution χ_3 mass, part 2. Individual GRACE based estimates (turquoise) for GravIS (dashed), GFZ RL06-SLR_TN11 (dotted) using the $\Delta C20$ replacement SLR_TN11 and GFZ RL06-SLR_GFZ (solid) using SLR_GFZ, like in GravIS. Orange X and circle defines the unweighted average incl. spread of all three GRACE based estimates. Individual SLR estimates (black) based on $\Delta C20$ from a multi-satellite solution (solid), the low degree replacement for GRACE GSM (dashed), and results published by Zhang (2017) (dotted). Black X and circle defines the unweighted average incl. spread of all three SLR estimates. The average and spread of all satellite (GRACE and SLR) estimates together leads to the mean mass term estimate (brown). For comparison the ESMGFZ model estimate is given in purple. Amplitudes are in milliseconds, phases are defined as φ in $\sin(\omega(t - t_0) + \varphi)$, where t_0 refers to 0 UTC on January 1 and $\omega = 1/365.25d$.

5. ANNUAL MOTION TERM VARIABILITY

On seasonal-to-interannual time-scales, the motion term contributions to ΔLOD are clearly dominated by tropospheric winds (Figure 3). OAM current contributions as simulated by MPIOM are almost two magnitudes smaller. AAM motion terms of ESMGFZ and AER agree very well in their annual phase, ± 2 days. Annual amplitudes of ECMWF-based estimates are lower by about 7% than NCEP results. In addition the annual amplitude – but not the semi-annual amplitude – of NCEP $\chi_{3,motion}$ depends considerably on the analysis period. NCEP gradually converges from $49.11 \cdot 10^{-10}$ (for the years 2000 - 2016) down to $47.01 \cdot 10^{-10}$ (for the years 1990 - 2000), towards the ECMWF level.

As AAM motion terms are two magnitudes larger than the second largest contribution from OAM, an alternative access to AAM $\chi_{3,motion}$ is given by subtracting the total mass contribution $\chi_{3,mass}$ discussed in the previous section from the geodetically observed excitation of ΔLOD .

We calculate two pseudo-observed $\chi_{3,motion}$ terms: (i) by using $\chi_{3,mass}$ terms from the sum of ESMGFZ EAMs; and (ii) by using the unweighted average of all GRACE and SLR estimates

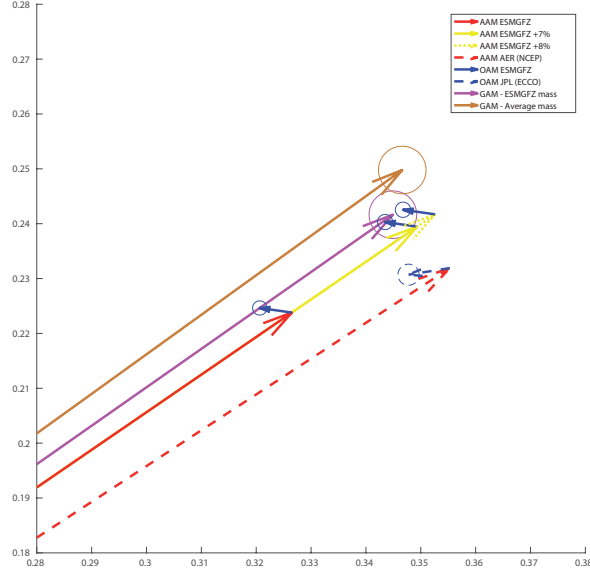


Figure 3: Phasor plot of annual motion term contribution χ_3 motion. Contributions of atmospheric winds (red) from ESMGFZ ECMWF (solid) and AER NCEP (dashed). Contributions of ocean currents (blue) from ESMGFZ MPIOM (solid) and JPL ECCO (dashed). Contributions of enhanced atmospheric winds (yellow) from ESMGFZ ECMWF + 7% (solid) and from ESMGFZ ECMWF + 8% (dotted). Pseudo-observation using GAM (IERS C04) reduced by the ESMGFZ mass term (purple) and the average mass term from GRACE/SLR satellite solutions (brown). Amplitudes are in milliseconds, phases are defined as φ in $\sin(\omega(t - t_0) + \varphi)$, where t_0 refers to 0 UTC on January 1 and $\omega = 1/365.25d$. Circles represent the uncertainties in estimating the annual harmonic signal.

discussed above. The uncertainties arising from the differences of those two mass term estimates account only for 2% in the annual amplitude of $\chi_{3,motion}$ and almost no uncertainty in the annual phase. Hence, the match between pseudo-observed and modeled $\chi_{3,motion}$ terms represents to a large extent the ability of the numerical weather models to capture the seasonal wind variations. By introducing a scaling factor that linearly increases the ECMWF wind terms by +7% we are able to obtain a remarkable closure of the IERS C04 Δ LOD excitation budget for the ESMGFZ mass term combination. When using the mass term estimates from GRACE/SLR, the ECMWF wind terms appear to be underestimated by even 8% or more, and also the NCEP wind terms are some 2% too low.

6. CONCLUSION

In order to validate the atmospheric motion excitation as calculated from predicted winds of numerical weather models against geodetic observation of Earth rotation, we first assess all other contributions coming from mass redistributions within the Earth system components atmosphere, ocean, and continental hydrosphere. Especially, the interactions between this subsystems via the global hydrological cycle cause substantial mass redistributions among atmosphere, ocean and continents.

Alternatively to the sum off all mass induced geophysical fluid excitation functions AAM, OAM, HAM, and SLAM, we used estimates of the Δ LOD mass term derived from satellite missions GRACE and SLR. GRACE based solution are very sensitive to the applied Δ C20 replacement derived from two different SLR solutions. This considerable diversity in SLR Δ C20 estimates is further supported by three more SLR solutions considered in this study. Nevertheless, the mass terms can be determined accurate enough from the ESMGFZ model combination as well as from

an average of all satellite based $\Delta C20$ solutions to attribute the mismatch between modeled and observed seasonal ΔLOD excitation clearly to the modeled motion terms. Especially ECMWF tends to underestimate strong atmospheric winds by -7%.

The conclusion of underestimated atmospheric winds is also supported by several studies comparing upper air wind predictions from numerical weather models with commercial aviation data. Applying a constant multiplier (presently set at 1.04) to the wind speeds forecasted by the Met Office the flight time errors are best minimized. Likely, assimilation systems used at the major weather operational centers (e.g. ECMWF, NCEP) tend to smooth sharp gradients, especially near the strong jets, resulting in too weak jet streaks by -5% to -9% (Cardinali et al., 2004).

7. REFERENCES

- Cardinali, C., Rukhovets, L. & Tenenbaum, J., 2004, "Jet Stream Analysis and Forecast Errors Using Aircraft Observations in the DAO, ECMWF, and NCEP Models", *Monthly Weather Review* 132, American Meteorological Society, pp. 764–779.
- Cheng, M. K., Tapley, B. D. & Ries, J. C., 2013, "Deceleration in the Earth's oblateness", *J. Geophys. Res. (Solid Earth)*, V118, pp. 1–8, doi:10.1002/jgrb.50058.
- Cheng, M., Ries, J. C. & Tapley, B. D., 2011, "Variations of the Earth's Figure Axis from Satellite Laser Ranging and GRACE", *J. Geophys. Res. (Solid Earth)* 116, B01409, doi: 10.1029/2010JB000850.
- Dahle, C., Flechtner, F., Murböck, M., Michalak, G., Neumayer, K., Abrykosov, O., Reinhold, A. & König, R., 2018, "GRACE 327-743 (Gravity Recovery and Climate Experiment): GFZ Level-2 Processing Standards Document for Level-2 Product Release 06 (Rev. 1.0, October 26, 2018)", Scientific Technical Report STR - Data, 18/04, Potsdam : GFZ German Research Centre for Geosciences, 20 p., doi: 10.2312/GFZ.b103-18048.
- König, R., Fagiolini, E., Raimondo, J. & Vei, M., 2018, "A Non-tidal Atmospheric Loading Model: On Its Quality and Impacts on Orbit Determination and C20 from SLR", – In: Freymueller, J. T., Sánchez, L.(Eds.), *International Symposium on Earth and Environmental Sciences for Future Generations : Proceedings of the IAG General Assembly, Prague, Czech Republic, June 22- July 2, 2015*, (International Association of Geodesy Symposia ; 147), Springer, pp. 189–194. doi:10.1007/1345_2016_257.
- Tamisiea, M. E., Hill, E. M., Ponte, R. M., Davis, J. L., Velicogna, I. & Vinogradova, N. T., 2010, "Impact of self-attraction and loading on the annual cycle in sea level", *J. Geophys. Res. (Oceans)* 115(C7), pp. 1–15., doi:10.1029/2009JC005687.
- Zhang, X., Jin, S., & Lu, X., 2017, "Global surface mass variations from continuous GPS observations and satellite altimetry data", *Remote Sensing* 9(10), doi:10.3390/rs9101000.